Homoharringtonine inhibits allergic inflammations by regulating NF-$\varkappa$B-miR-183-5p-BTG1 axis

Misun Kim[1], Hyein Jo[1], Yoojung Kwon[1], Youngmi Kim[2], Hyun Suk Jung[1], and Dooil Jeoung[3]

[1]Kangwon National University
[2]Hallym University College of Medicine
[3]Kangwon National University, College of National Science

May 5, 2020

Posted on Authorea 20 Feb 2020 — CC BY 4.0 — https://doi.org/10.22541/au.158221349.94174215 — This a preprint and has not been peer reviewed. Data may be preliminary.

Abstract

BACKGROUND AND PURPOSE: Homoharringtonine (HHT) is a drug for treatment of chronic myeloid leukemia. This study investigated the role of homoharringtonine in allergic inflammations. EXPERIMENTAL APPROACH: Mouse model of atopic dermatitis (AD) induced by DNFB and anaphylaxis employing DNP-HSA were used to examine the role of homoharringtonine in allergic inflammations. We investigated roles of miR-183-5p, regulated by HHT in RBL2H3 cells, in AD and anaphylaxis. KEY RESULTS: HHT exerted negative effects on in vitro allergic inflammation and attenuated clinical symptoms associated with AD. AD increased the expression levels of hallmarks of allergic inflammation and induced features of allergic inflammation in rat basophilic leukemia (RBL2H3) cells. HHT prevented DNFB from increasing the expression of Th1/Th2 cytokines in mouse model of AD. HHT inhibited passive cutaneous anaphylaxis and passive systemic anaphylaxis. MiR-183-5p inhibitor inhibited anaphylaxis and AD. B cell translocation gene 1 (BTG1) was shown to be a direct target of miR-183-5p. BTG1 prevented antigen from inducing molecular features of in vitro allergic inflammation. AD increased the expression of NF-kB, and NF-kB showed binding to the promoter sequences of miR-183-5p. NF-kB and miR-183 formed positive feedback to mediate in vitro allergic inflammation. Curcumin inhibited in vitro allergic inflammation and attenuated AD by regulating the expression levels of miR-183-5p and BTG1. Curcumin and miR-183-5p inhibitor prevented cellular interactions involving mast cells and macrophages in AD. CONCLUSIONS AND IMPLICATIONS: HHT can be developed as anti-allergy drug and NF-$\varkappa$B- miR-183-5p-BTG1 axis can serve as a target for the development of anti-allergy drugs.

Abbreviations

AD, atopic dermatitis; BTG1, B cell translocation gene 1; DNFB, 2, 4,-dinitrofluorobenzene; DNP-HSA, 2,4-dinitrophenyl human serum albumin; H&E, hematoxylin and eosin; HHT, Homoharringtonine; miRNA, microRNA; PCA, passive cutaneous anaphylaxis; PSA, passive systemic anaphylaxis; RBL2H3, rat basophilic leukemia; UTR, untranslated region

Keywords: Anaphylaxis; Atopic dermatitis; Homoharringtonine; miR-183-5p; NF-kB

Running title: Anti-allergic effect of homoharringtonine

Introduction

Homoharringtonine (HHT), a protein translation inhibitor of plant alkaloid, exhibits cytotoxic effect against acute myeloid leukemia cell lines. HHT shows cytotoxic effects against acute lymphoblastic leukemia (ALL) cells and chronic myeloid leukemia (CML) cells by decreasing expression of Bcl-6 (Wang *et al.,* 2017). It inhibits tumorigenic potential of gefitinib-resistant non-small cell lung cancer cells (Cao*et al.,* 2015), inhibits infiltration of imatinib-resistant mast tumor cells harboring imatinib-resistant D814Y KIT gene (Jin *et al.,*

2010) and the in vitro growth of triple-negative breast cancer cells by decreasing expression levels of anti-apoptotic proteins such as Bcl-2, survivin and X-linked inhibitor of apoptosis protein (XIAP) (Yakhni *et al.,* 2019). Bcl-XL, an anti-apoptotic protein, confers protection against cytotoxic effect of HHT in human leukemia cells (Lin*et al.,* 2011).

HHT in combination with hsp90 inhibitor IPI504 synergistically inhibits leukemia cells by exerting apoptotic effects (Wu *et al.,* 2019). Abivertinib, an inhibitor of Bruton's tyrosine kinase (BTK), in combination with HHT have synergistic effect in treating acute myeloid leukemia cells (Huang *et al.,* 2019). HHT in combination with bortezomib exert cytotoxic effects against diffuse large B cell lymphoma (DLBCL) and mantle cell lymphoma (MCL) cells by myeloid leukemia cell differentiation protein-1 (MCL-1) down-regulation, Phorbol-12-Myristate-13-Acetate-Induced Protein 1 (PMAIP1) up-regulation, and Bcl-2 homologous antagonist/killer (BAK) activation (Nguyen *et al.,* 2018).

HHT binds to NF-ϰB repressing factor (NKRF). Second double-strand RNA-binding motif (DSRM2) domain of NKRF is necessary for binding of HHT to NKRF. HHT shifts NKRF from the nucleus to the cytoplasm, strengthens the p65-NKRF interaction, and interferes with p65-p50 complex formation, thereby attenuating the transactivation activity of p65 on the*MYC* gene (Chen *et al.,* 2019b). HHT binds to myosin-9. The increased expression level of myosin-9 is correlated with enhanced apoptotic effect of HHT (Zhang *et al.,* 2016). HHT decreases the expression of *KIT* , a frequently mutated and/or highly expressed gene in t (8; 21) Acute Myeloid Leukemia (AML), in concert with MYC down-regulation (Chen *et al.,* 2019b).

In this study, we examined roles of HHT in allergic inflammations. HHT attenuated atopic dermatitis (AD) and exerted negative effects on anaphylaxis. MiR-183-5p was one of those miRNAs that was regulated by HHT during in vitro allergic inflammation. MiR-183-5p was shown to mediate AD and anaphylaxis. NF-kB was responsible for the increased expression of miR-183-5p during allergic inflammation. BTG1served as a target of miR-183-5p and inhibited in vitro allergic inflammation. Anti-atopic and anti-anaphylactic effects of HHT have not been reported. The mechanisms of anti-allergic effects by HHT merit further investigation. We provided evidence that HHT can be developed as anti-allergy drug and that miR-183-5p-BTG1 axis can be a target for the development of anti-allergy drugs.

Methods

Animals

Female BALB/C mice that were five week old were purchased from Nara Biotech (Seoul, South Korea) and were group housed under specific pathogen-free conditions in the animal facility of the Kangwon National University. All animal experiments were approved by Institutional Animal Care and Use Committee (IACUC) of Kangwon National University (KW180823-1).

Materials

2, 4-dinitrofluorobenzene (DNFB) was purchased from Sigma-Aldrich (St. Louis, MO, United States). All other chemicals used in this study were also purchased from Sigma-Aldrich (St. Louis, MO, United States). The following antibodies were obtained from Santa Cruz Biotechnology (Dallas, TX, United States): histone deacetylase 3 (HDAC3), cyclooxygenase-2 (COX-2), monocyte chemoattractant protein 1 (MCP1), Lyn, SOCS1, Fc?RIβ, and actin. Anti-mouse and anti-rabbit IgG horseradish peroxidase (HRP)-conjugated antibodies were purchased from Thermo Pierce (Rockford, IL, United States). The jetPRIME transfection reagent was purchased from Polyplus (NY, United States). The miRNA inhibitor was purchased from Bioneer Company (Daejeon, South Korea). Primers used in this study were commercially synthesized by Bioneer Company (Daejeon, South Korea). The chemical library used in this study was kindly provided by Korea Chemical Bank of Korea Research Institute of Chemical Technology.

Cell Culture

Isolations of mast cells and macrophages were performed according to the standard procedures with slight modifications (Eom *et al.,* 2014). Rat basophilic leukemia (RBL2H3) cells were obtained from the Korea Cell

Posted on Authorea 20 Feb 2020 — CC BY 4.0 — https://doi.org/10.22541/au.158221349.94174215 — This a preprint and has not been peer reviewed. Data may be preliminary.

Line Bank (Seoul, South Korea). Cells were grown in DMEM containing heat-inactivated fetal bovine serum, 2 mM L-glutamine, 100 U/ml penicillin, and 100 μg/ml streptomycin (Invitrogen). Cultures were maintained in 5% CO_2 at 37°C. Human keratinocyte HaCaT cells were purchased (HDFa lot #1780051, Gibco, Grand Island, NY, United States) and expanded in Dulbecco's modified eagle medium (DMEM; Gibco, Grand Island, NY, United States) containing 8% fetal bovine serum (Gibco, Mulgrave Victoria, Australia) at 37°C with 5% CO_2.

β-Hexosaminidase Activity Assays

β-hexosaminidase activity assays were performed according to the standard procedures (Noh*et al.,* 2017).

Immunoblot and Immunoprecipitation

Immunoblot and immunoprecipitation were performed according to the standard procedures (Noh *et al.,* 2017).

MiRNA Array Analysis

The miRNA expression analysis was performed by using miRNA Array III kit (Signosis, CA, United States) following the manufacturer's instructions. Five μg of total miRNA was annealed to an oligonucleotide primer mix and hybridized to 132 miRNA oligonucleotide probes. Streptavidin-HRP chemiluminescence was used for the detection of miRNA expression.

MiRNA Target Analysis

Genes that contain the miR-binding site(s) in the untranslated region (UTR) were obtained using the TargetScan program.

MiRNA Extraction and Quantitative Real-Time PCR

Total miRNA was isolated with the miRNeasy Micro Kit (Qiagen, CA, United States) following the standard protocol from the manufacturer. The extracted miRNA was reverse transcribed using a miScript II RT Kit (Qiagen, CA, United States) with universal RT primer. The expression level of miR-183-5p was quantified with SYBR Green Master Mix (Qiagen, CA, United States) using a miRNA-specific forward primer and universal reverse primer. Relative expression of miRNA was calculated using the $2^{-\Delta\Delta^{\sim}T}$ method ($\Delta CT = CT_{miR}\text{-}CT_{reference}$). The U6 small nuclear RNA was used as an endogenous control for data normalization. The expression levels of T-helper 1 (Th1)/T-helper 2 (Th2) cytokines and BTG1 were also quantified by quantitative real-time PCR (qRT-PCR) analysis.

Transfection

Transfections were performed according to the manufacturer's instructions. Lipofectamine and Plus reagents (Invitrogen) were used. For miR-183-5p knockdown, cells were transfected with 10 nM oligonucleotide (inhibitor) with Lipofectamine 2000 (Invitrogen), according to the manufacturer's protocol. The sequences used were 5'-AGUGAAUUCUACCAGUGCCAUA -3' (miR-183-5p inhibitor) and 5'-TAACACGTCTATACGCCCA -3' (control inhibitor).

Luciferase activity assays

To generate the pGL3 3'-UTR-BTG1 construct, a 947-bp mouse BTG1 gene segment encompassing 3'-UTR was PCR-amplified and subcloned into the XbaI site of pGL3 luciferase plasmid. The mutant pGL3 3'-UTR-BTG1 construct was made with the Quick Change site-directed mutagenesis kit (Stratagene). Luciferase activity assay was performed according to the instruction manual (Promega).

pFlag-BTG1construct was made by PCR amplification and cloning into Flag-tagged pcDNA3.1 vector.

Chromatin Immunoprecipitation Assays

Assays were performed according to manufacturer's instruction (Upstate). For detection of the binding of protein of interest to miR-183-5p promoter sequences, specific primers of miR-183-5p promoter-1 sequences [5'-

Posted on Authorea 20 Feb 2020 — CC BY 4.0 — https://doi.org/10.22541/au.158221349.94174215 — This a preprint and has not been peer reviewed. Data may be preliminary.

GGCCCAGAATCTACTGATAGTG -3' (sense) and 5'- TAAGTCTCTCTGGAGCTGGTG -3' (antisense)], miR-183-5p promoter-2 sequences [5'- CACCAGCTCCAGAGAGACTT -3' (sense) and 5'- AGAGGCCCA-GAAGGTAAGAC -3' (antisense)], miR-183-5p promoter-3 sequences [5'- GTCTTACCTTCTGGGCCTCT -3' (sense) and 5'- GACTGATTTCTTGGGTTTGCAG -3' (antisense)], and miR-183-5p promoter-4 sequences [5'- AGCCCCGTCTTTCTCCTT -3' (sense) and 5'- CAGACCCTACAGAGAGGTCA -3' (antisense)] were used.

Histological Examination

Skin samples were collected, fixed with 10% neutral buffered formalin, and embedded in paraffin. Sections (5 μm thickness) were prepared and stained with haemotoxylin and eosin (H&E) or toluidine blue for leukocyte infiltration or mast cell infiltration and degranulation, respectively.

Immunohistochemical Staining

Immunohistochemical staining of tissues was performed using an established avidin-biotin detection method (Vectastain ABC kit, Vector Laboratories Inc., Burlingame, CA, United States). 4–6 μm-thick sections of the paraffin-embedded tissue blocks were cut, mounted on positively charged glass slides, and dried in an oven at 56°C for 30 min. The sections were deparaffinized in xylene and then rehydrated in graded ethanol and water. Endogenous peroxidase was blocked by incubation in 3% (v/v) hydrogen peroxide for 15 min. Antigen retrieval was accomplished by pretreatment of the sections with citrate buffer at pH 6.0 for 20 min at 56°C in a microwave oven, and then the sections were allowed to cool for 30 min. Nonspecific endogenous protein binding was blocked using 1% bovine serum albumin (BSA). The sections were then incubated with primary antibodies overnight at 4°C. The following primary antibodies were used: anti-HDAC3 (1:100, Santa Cruz Biotechnology); anti-MCP1 (1:100, Invitrogen); anti-CD163 (1: 700, Abcam); anti-TSLP (1:500, Abcam); anti-BTG1 (1:200, Abcam), and anti-inducible nitric oxide synthase (iNOS) (1: 500, Santa Cruz Biotechnology). After washing, biotinylated secondary antibodies were applied at 1:100 or 1:200 dilutions for 1 h. Color was developed with diaminobenzidine (Vector Laboratories, Inc.). Sections were counterstained with Mayer's hematoxylin. The sections incubated without primary antibody served as controls. To visualize tissue mast cells, the sections were stained with 0.1% toluidine blue (Sigma) in 0.1 N HCl for 15 min.

Immunofluorescence staining

Cells were seeded onto glass coverslips in 24-well plates and were fixed with 4% paraformaldehyde (v/v) for 10 min and then permeabilized with 0.4% Triton X-100 for 10 min. Cells were incubated with primary antibody specific to CD163 (1:100; Abcam), iNOS (1:100; Santa Cruz Biotechnology), or NF-kB (1:200, Cell signaling Technology) for 2 h. Anti-rabbit Alexa Fluor 488 (for detection of iNOS) or anti-goat Alexa Fluor 546 (for detection of CD163 and NF-kB) secondary antibody (Molecular Probes) was added to cells and incubated for 1 h. Fluorescence images were acquired using a confocal laser scanning microscope and software (Fluoview version 2.0) with a X 60 objective (Olympus FV300, Tokyo, Japan).

Induction of Atopic Dermatitis in BALB/C Mice

Symptoms of atopic dermatitis (AD) were induced by using DNFB, as previously described (Kwon et al., 2010), with minor modifications. Briefly, the upper backs of the mice were shaved with a clipper. After 24 h, 150 μl of 1% DNFB in acetone: olive oil mixture (3:1 vol/vol) was topically applied on days 1 through 8. Later, the same dose of 0.2% DNFB was applied four times a week. Dermatitis scores of 0 (none), 1 (mild), 2 (moderate), and 3 (severe) were given for each of the four symptoms: dryness, excoriation, erosion, and erythema and edema. The sum of the individual scores was used as the clinical severity.

Passive Cutaneous Anaphylaxis (PCA)

The BALB/C mice were sensitized with an intradermal injection of 2, 4-dinitrophenol (DNP)-specific IgE (0.5 μg/kg). After 24 h, the mice were challenged with an intravenous injection of DNP-human serum albumin (HSA) (250 μg/kg) and 2% (v/v) Evans blue solution. After 30 min of DNP-HSA challenge, the mice were euthanized, and the 2% (v/v) Evans blue dye was extracted from each dissected ear in 700 μl of acetone/water

Posted on Authorea 20 Feb 2020 — CC BY 4.0 — https://doi.org/10.22541/au.158221349.94174215 — This a preprint and has not been peer reviewed. Data may be preliminary.

(7:3) overnight. The absorbance of Evans blue in these extracts was measured with a spectrophotometer at 620 nm. To determine the effect of miR-183-5p on the PCA, BALB/C mice were given an intradermal injection of IgE (0.5 μg/kg) and intravenous injection of the indicated inhibitor (each at 100 nM). The next day, BALB/C mice were given an intravenous injection of PBS or DNP-HSA (250 μg/kg) along with 2% (v/v) Evans blue solution for determining the extent of vascular permeability accompanied by PCA. Later, 1 h after the injection of Evans blue solution, the dye was eluted from the ear in 700 μl of formamide at 63°C. The absorbance was measured at 620 nm.

Passive Systemic Anaphylaxis (PSA)

To determine effect of miR-183-5p on passive systemic anaphylaxis, BALB/C mice were given an intravenous injection of control inhibitor (100 nM) or miR-183-5p inhibitor (100 nM). The next day, BALB/C mice were sensitized by intravenous injection of IgE (0.5 μg/kg). The next day, the sensitized mice were intravenously injected with DNP-HSA (250 μg/kg). Changes in core body temperature associated with systemic anaphylaxis were monitored by measuring changes in rectal temperatures using a rectal probe coupled to a digital thermometer.

Statistical Analysis

Data were analyzed and graphed using the GraphPad Prism statistics program (GraphPad Prism software). Results are presented as means ± SE. Statistical analysis was performed using t -tests with differences between means considered significant when $p < 0.05$.

Results

HHT inhibits in vitro allergic inflammation

To identify the chemical compounds that inhibit allergic inflammations, we screened chemical library, consisting of 1019 chemicals derived from natural products. We hypothesized that chemicals that inhibit β-hexosaminidase activity would negatively affect in vitro and in vivo allergic inflammations. We identified several compounds that prevented antigen (DNP-HSA) from increasing β-hexosaminidase activity in rat basophilic leukemia cells (RBL2H3). Among these compounds, homoharringtonine (HHT) showed the most potent effect against β-hexosaminidase activity (data not shown). HHT activates the TGF-β pathway via phosphorylation of smad3 (Ser423/425 (Chen *et al.*,2017). TGF-β inhibits allergic inflammation (Noh *et al.,* 2017). We therefore hypothesized that HHT might affect allergic inflammation. HHT, in a dose-dependent manner, prevented antigen from increasing levels of hallmarks of allergic inflammation such as HDAC3, SOCS1 and TGaseII in RBL2H3 cells (Figure 1A). HHT also prevented antigen from increasing expression levels of HDAC3, SOCS1 and TGaseII in lung mast cells (Figure 1A). HHT prevented antigen from inducing interactions of FcεRI with Lyn and HDAC3 (Figure 1B) and prevented antigen from increasing the β-hexosaminidase activity in RBL2H3 cells (Figure 1C). The regulatory role of HHT in in vitro allergic inflammation has not been reported.

HHT inhibits anaphylaxis

HHT exerted a negative effect on passive cutaneous anaphylaxis (PCA) employing BALB/C mouse (Figure 2A). HHT prevented antigen (DNA-HSA) from increasing β-hexosaminidase activity (Figure 2B). HHT prevented antigen from increasing levels of hallmarks of allergic inflammations and from inducing interactions of FcεRI with Lyn, HDAC3, and SOCS1 (Figure 2C).

HHT prevented DNP-HSA from reducing rectal temperature in BALB/C mouse model of passive systemic anaphylaxis (PSA) (Figure S1A). HHT prevented antigen from increasing β-hexosaminidase activity (Figure S1B) and levels of hallmarks of allergic inflammations (Figure S1C), and from inducing interactions of FcεRI with Lyn and SOCS1 (Figure S1C). Immunohistochemical staining showed that HHT alos prevented antigen from increasing expression of HDAC3 (Figure S1D).

HHT inhibits AD

Posted on Authorea 20 Feb 2020 — CC BY 4.0 — https://doi.org/10.22541/au.158221349.94174215 — This a preprint and has not been peer reviewed. Data may be preliminary.

AD shares common molecular features with anaphylaxis (Kim *et al.,*2018a). We examined the effect of HHT on AD. HHT attenuated clinical symptoms associated with AD induced by 2, 4,-dinitrofluorobenzene (DNFB) (Figure 3A). HHT prevented AD from increasing levels of hallmarks of allergic inflammations, such as thymic stromal lymphopoietin protein (TSLP), COX2, MCP1, and CXCL10 (Figure 3D). TSLP is a marker of AD. AD is closely related with the increased production of Th1 cytokines such as CXCL10 (Brunner *et al.,* 2017). HHT prevented AD from regulating expression levels of CD163 and iNOS, markers of M1 (classical) and M2 macrophages (alternative), respectively (Figure 3D), and from inducing interactions of FcεRI with Lyn, HDAC3, and SOCS1 (Figure 3D). Mast cells were isolated from skin tissues of BALB/C mice under AD without or with HHT treatment. Immunoblot and immunoprecipitation showed that HHT exerted negative effects on molecular features associated with AD (Figure 3E). AD increased expression levels of T-bet and GATA, but decreased expression of FoxP3 (Figure 3F). T-bet and GATA-3 are transcriptional factors of Th1 cells and Th2 cells, respectively. Foxp3 is a specific transcriptional factor of Treg cells. HHT prevented AD from increasing expression levels of HDAC3 and MCP1 (Figure S2A), regulating expression levels of iNOS and CD163 (Figure S2A), inducing epidermal hyperplasia (Figure S2B) and increasing number of activated mast cells (Figure S2B). It also prevented DNFB from increasing β-hexosaminidase activity (Figure 3B) and the amount of histamine released (Figure 3C). We examined whether DNFB, just like DNP-HSA, would induce features of allergic inflammation. DNFB increased levels of hallmarks of allergic inflammation and induced interactions of FcεRI with Lyn and HDAC3 in RBL2H3 cells (Figure S3). HHT prevented DNFB from inducing features of in vitro allergic inflammation (Figure S3). Thus, HHT attenuates clinical symptoms associated with AD by regulating molecular features of allergic inflammation.

HHT prevents AD from regulating expression of cytokines

Increased expression levels of T_H1 (IFN-γ), T_H2 (IL-31), and T_H17/T_H22 (IL-23p19/IL-8/S100A12) mRNA expression are closely related with human AD (Guttman-Yassky *et al.,* 2019). AD increased expression levels of Th1 cytokines such as IL-1β, IFN-γ and TNF-α (Figure S4). AD increased expression levels of Th2 cytokines such as IL-4, IL-5, IL-6, and IL-13 (Figure S4). AD decreased expression levels of FoxP3 and IL-10 (Figure S4). HHT prevented AD from regulating expression levels of these cytokines. Thus, HHT inhibits AD by regulating expression levels of inflammatory cytokines.

.

MiR-183-5p mediates in vitro allergic inflammation

Various studies have reported the roles of miRNAs in allergic inflammations (Nimpong *et al.,* 2017; Kim *et al.,* 2019). MiRNA array analysis was performed to identify miRNAs that were regulated by HHT in RBL2H3 cells (Figure 4A). Among these, miR-183-5p was clearly upregulated by antigen stimulation and decreased by HHT in RBL2H3 cells (Figure 4A). MiR-183-5p is a biomarker of occupational asthma (OA) (Lin *et al.,* 2019). QRT-PCR analysis showed that HHT prevented antigen from increasing expression of miR-183-5p in RBL2H3 cells and lung mast cells (Figure 4B). MiR-183-5p inhibitor prevented antigen from increasing β-hexosaminidase activity (Figure 4C) and prevented antigen from increasing levels of hallmarks of allergic inflammation in RBL2H3 cells (Figure 4D). MiR-183-5p inhibitor prevented antigen from inducing interactions of FcεRI with HDAC3, Lyn, and SOCS1 (Figure 4D). Thus, miR-183-5p is necessary for in vitro allergic inflammation.

MiR-183-5p mediates anaphylaxis

MiR-183-5p inhibitor exerted a negative effect on PCA (Figure 5A). PCA increased the expression of miR-183-5p at the transcriptional level (Figure 5B). MiR-183-5p inhibitor prevented PCA from increasing β-hexosaminidase activity and the amount of histamine released in BALB/C mice (Figure 5B), increasing levels of hallmarks of allergic inflammation and CD163, however, prevented antigen from decreasing expression of iNOS (Figure 5C). MiR-183-5p inhibitor also prevented PCA from inducing interactions of FcεRI with HDAC3, Lyn, and SOCS1 (Figure 5C). MiR-183-5p inhibitor prevented antigen from decreasing rectal temperatures in BALB/C mouse model of PSA (Figure S5A) and from increasing β-hexosaminidase activity in BALB/C mice (Figure S5B). PSA increased the expression of miR-183-5p at the transcriptional level

Posted on Authorea 20 Feb 2020 — CC BY 4.0 — https://doi.org/10.22541/au.158221349.94174215 — This a preprint and has not been peer reviewed. Data may be preliminary.

(Figure S5B). MiR-183-5p inhibitor prevented antigen from increasing levels of hallmarks of allergic inflammation and CD163 but prevented antigen from decreasing expression of iNOS (Figure S5C). MiR-183-5p inhibitor also prevented PSA from inducing interactions of FcεRI with HDAC3, Lyn, and SOCS1 (Figure S5C). Thus, miR-183-5p mediates anaphylaxis.

MiR-183-5p mediates AD

MiR-183-5p inhibitor attenuated clinical symptoms associated with AD (Figure 6A). MiR-183-5p inhibitor prevented DNFB from increasing β-hexosaminidase activity (Figure 6B), increasing levels of hallmarks of allergic inflammation and CD163, and from decreasing expression of iNOS (Figure 6C). MiR-183-5p inhibitor prevented DNFB from inducing interactions of FcεRI with HDAC3, Lyn, and SOCS1 (Figure 6C). AD increased expression levels of IL-1β, IL-2, IL-5, IL-6, IL-8, IL-17, and IFN-γ in BALB/C mouse in miR-183-5p-dependent manner (Figure 6D). miR-183-5p inhibitor prevented DNFB from increasing expression levels of HDAC3, MCP1, and CD163, and decreasing expression of iNOS (Figure S6A). Toluidine blue staining showed that miR-183-5p inhibitor prevented DNFB from increasing number of activated mast cells (Figure S6B). H&E staining showed that miR-183-5p inhibitor prevented DNFB from inducing skin hyperplasia (Figure S6B). Thus, miR-183-5p mediates AD by regulating molecular and cellular features associated with AD.

NF-kB regulates expression of miR-183-5p

HHT binds to NF-kB repressing factor (Chen *et al.,* 2019b). AD induces activation of NF-kB signaling in Nc/Nga mouse model (Sung*et al.,* 2018). PCA activates of NF-ϰB signaling (Kang *et al.,* 2019). MAPK, PI3K/AKT, and NF-kB function as downstream signaling pathways of FcεRI (Ye *et al.,* 2017). We therefore examined whether NF-kB would be involved in the expression regulation of miR-183-5p. HHT and miR-183-5p inhibitor prevented DNFB from increasing the expression of NF-kB in BALB/C mouse model of AD (Figure S7A). HHT also prevented DNFB from increasing expression of NF-kB in RBL2H3 cells (Figure S7A). TLR2 activates mast cells and mediates AD (Tsurusaki*et al.,* 2016). NF-kB signaling is necessary for TLR2 ligand–mediated skin inflammation (Jiao *et al.,* 2016). DNFB increased the expression of TLR2 in BALB/C mouse and RBL2H3 cells (Figure S7A). HHT and miR-183-5p inhibitor prevented DNFB from increasing expression of TLR2 in BALB/C mouse (Figure S7A). HHT also prevented DNFB from increasing expression of TLR2 in RBL2H3 cells (Figure S7A). BAY11-7082, an inhibitor of NF-kB, prevented DNFB from inducing nuclear translocation of NF-kB in RBL2H3 cells (Figure S7B). ChIP assay showed binding of NF-kB to the promoter sequences of miR-183-5p (Figure S7C). Thus, NF-kB and miR-183-5p form a positive feedback loop to mediate AD.

BTG1 acts as negative regulator of allergic inflammation

TargetScan analysis predicted BTG1 as a target of miR-183-5p. Luciferase activity assays showed that miR-183-5p directly regulated the expression of BTG1 (Figure S8A). HHT and miR-183-5p inhibitor prevented DNFB from decreasing the expression of BTG1 in BALB/C mouse model of AD (Figure S8B). HHT prevented antigen from decreasing the expression of BTG1 in RBL2H3 cells (Figure S8C). Overexpression of BTG1 prevented antigen from increasing levels of hallmarks of allergic inflammation (Figure 7A), prevented antigen from inducing interactions of FcεRI with HDAC3, Lyn, and SOCS1 (Figure 7A), and prevented antigen from increasing β-hexosaminidase activity and the expression of miR-183-5p in RBL2H3 cells (Figure 7B). DNFB decreased the expression of BTG1 in HaCaT cells (Figure 7C). Overexpression of BTG1 prevented DNFB from increasing levels of hallmarks of allergic inflammation and miR-183-5p in HaCaT cells (Figure 7C). Thus, BTG1, a target of miR-183-5p, acts as a negative regulator of in vitro allergic inflammation.

NF-kB mediates in vitro and in vivo allergic inflammation

TLR4-NF-kB signaling is necessary for maintaining epithelial barrier in allergic inflammation (Tao *et al.,* 2017). BAY11-7082, an inhibitor of NF-ϰB, prevented antigen from increasing expression levels of NF-kB, pIkB^{Ser32}, TLR2, and TLR4 (Figure 8A), decreasing the expression level of BTG1 in RBL2H3 cells

Posted on Authorea 20 Feb 2020 — CC BY 4.0 — https://doi.org/10.22541/au.158221349.94174215 — This a preprint and has not been peer reviewed. Data may be preliminary.

(Figure 8A). BAY11-07082 also prevented antigen from inducing interactions of FcεRI with Lyn, HDAC3, and SOCS1 (Figure 8A). BAY11-7082 prevented antigen from increasing the expression level of miR-183-5p and β-hexosaminidase activity (Figure 8B). BAY11-7082 rather increased the expression level of BTG1 at the transcriptional level in unstimulated RBL2H3 cells and prevented antigen from significantly decreasing the expression of BTG1 at the transcriptional level (Figure 8B). BAY11-7082 prevented antigen from inducing nuclear translocation of NF-kB (Figure 8C). BAY11-7082 prevented DNFB from increasing expression levels of $pIkB^{Ser32}$, hallmarks of allergic inflammation, and miR-183-5p (Figure 8D). BAY11-07082 prevented DNFB from decreasing the expression level of BTG1 in HaCaT cells (Figure 8D). BAY11-7082 exerted a negative effect on PCA (Figure S9A) and prevented PCA from increasing β-hexosaminidase activity and the expression levels of BTG1 and miR-183-5p at the transcriptional level (Figure S9B), increasing the expression levels of BTG1, NF-kB, and $pIkB\alpha^{Ser32}$(Figure S9C) and decreasing the expression level of BTG1 (Figure S9C). BAY11-7082 prevented DNFB from inducing nuclear translocation of NF-kB in HaCaT cells (Figure S9D).

Curcumin inhibits in vitro allergic inflammation by regulating expression levels of miR-183-5p and BTG1

Curcumin suppresses intestinal anaphylaxis by inhibiting NF-kB activation in ovalbumin-challenged allergic mice (Kinney *et al.*,2015). Curcumin inhibits PCA by regulating syk activity (Lee *et al.,* 2008). Curcumin prevented antigen from increasing levels of hallmarks of allergic inflammation, decreasing expression level of BTG1 in RBL2H3 cells (Figure S10A) and from increasing expression of miR-183-5p (Figure S10A). Curcumin prevented DNFB from increasing expression levels of NF-kB and hallmarks of allergic inflammation (Figure S10B), inducing interactions of FcεRI with HDAC3, Lyn, and SOCS1 in RBL2H3 cells (Figure S10B), and from decreasing the expression level of BTG1 in RBL2H3 cells (Figure S10B). Curcumin inhibited nuclear translocation of NF-ϰB by DNP-HSA (Figure S10C) and by DNFB (Figure S10D). Curcumin also prevented DNFB from decreasing the expression level of BTG1 (Figure S10E) and increasing the expression of miR-183-5p at the transcriptional level in HaCaT cells (Figure S10E).

Curcumin inhibits AD

The effect of curcumin on AD was examined. BALB/C mice were given an intraperitoneal injection of curcumin on days of the time line (Figure 9A). Curcumin attenuated clinical symptoms associated with AD (Figure 9A). Curcumin prevented DNFB from increasing β-hexosaminidase activity and the expression level of miR-183-5p (Figure 9B), decreasing expression of BTG1 at the transcriptional level (Figure 9B) and from increasing levels of hallmarks of allergic inflammation (Figure 9C). Curcumin also prevented DNFB from inducing interactions of FcεRI with Lyn and HDAC3 (Figure 9C). Immunoblot of skin mast cells isolated from BALB/C mouse under AD showed that curcumin prevented DNFB from decreasing expression level of BTG1 and increasing levels of hallmarks of allergic inflammation (Figure 9D). Curcumin prevented DNFB from decreasing expression level of BTG1, increasing expression levels of MCP1 and TSLP (Figure S11A), from increasing number of activated mast cells and from inducing skin hyperplasia (Figure S11B).

HHT and miR-183-5p regulate cellular interactions in AD

We examined whether cellular interactions would be necessary for AD. Culture medium of skin mast cells isolated from AD-induced BALB/C mouse increased expression levels of CD163 and hallmarks of allergic inflammation, but decreased the expression of iNOS in macrophages (Figure 10, A and B). HHT inhibited activation of macrophages by culture medium of mast cells from AD-induced BALB/C mouse (Figure 10, A and B). Culture medium of mast cells from AD-induced BALB/C mouse increased expression levels of CD163, but decreased expression levels of BTG1 and iNOS in macrophages (Figure S12, A and C). Culture medium of mast cells from AD-induced BALB/C mouse injected with miR-183-5p inhibitor had no significant effect on expression level of BTG1, CD163 or iNOS in macrophages (Figure S12, A and C). Culture medium of mast cells from AD-induced BALB/C mouse injected with curcumin had no significant effect on expression level of BTG1, CD163 or iNOS in macrophages (Figure S12, B and D). Thus, HHT and miR-183-5p inhibitor exert anti-atopic effect by inhibiting cellular interactions involving mast cells and macrophages.

Posted on Authorea 20 Feb 2020 — CC BY 4.0 — https://doi.org/10.22541/au.158221349.94174215 — This a preprint and has not been peer reviewed. Data may be preliminary.

Discussion

In this study, we showed that HHT prevented antigen from increasing expression of HDAC3 and inducing the interaction between FcεRI and HDAC3 in RBL2H3 cells. HDAC3 mediates allergic skin inflammation by increasing expression level of MCP1 and binds to FcεRI (Kim *et al.,* 2012). HDAC3 is necessary for enhanced tumorigenic and metastatic potential by allergic inflammation (Eom *et al.,* 2014b). HDAC3 exerts negative effect on the expression of HDAC2 in antigen-stimulated RBL2H3 cells (Kim *et al.,* 2012). For future studies, it would be necessary to examine effect of HHT on the expression levels of HDAC2 and other HDACs.

HHT prevented AD and anaphylaxis from increasing expression of SOCS1. SOCS1, decreased by TGFβ, mediates in vitro and in vivo allergic inflammation and binds to FcεRI (Noh *et al.,* 2017). SOCS1 forms a negative feedback loop with miR-122a-5p and mediates AD (Kim *et al.,* 2018a). It is reasonable that HHT may increase expression level of TGFβ and miR-122a-5p.

AD is accompanied by an increased expression levels of Th2 cytokines such as IL-4, IL-5, and IL-13 (Wang *et al.,* 2018). In mouse model of allergic lung disease, inhibition of pulmonary Th2 responses leads to increased production IL-10 (Nunes *et al.,* 2019). TSA, an inhibitor of HDACs, suppresses DNFB-induced AD by decreasing production of Th2 cytokines such as IL-4 (Kim *et al.,* 2010). We showed that AD increased expression levels of TH1/TH2 cytokines but decreased the expression of IL-10. It would be interesting to examine whether IL-10 would negatively regulate AD and anaphylaxis. HHT prevented AD from increasing expression level of IL-17. IL-17 is closely associated with asthma and AD development (Silva *et al.,* 2019). IL-17 allows F-actin to interact with myosin and is critical for the contraction of airway smooth muscle cells (Bulek *et al.,* 2019). Decreased expression of IL-17 leads to resolution of psoriasis (Krueger *et al.,* 2019). IL-17 is necessary for the pathogenesis of asthma including airway hyperresponsiveness (Bulek *et al.,* 2019). It would be necessary to examine whether IL-17 would regulate AD and anaphylaxis.

We examined the miRNAs that were regulated by HHT. MiR-183-5p was one of those miRNAs that were increased by antigen stimulation and downregulated by HHT in RBL2H3 cells. MiR-183-5p targets hemeoxygenase 1(HO-1) (Davis *et al,* 2017). HO-1 suppresses Th2 responses in a mouse model of ovalbumin-induced eosinophilic asthma and reduces apoptosis of primary airway epithelial cells (pAECs) (Lv *et al.,*2018a). Activation of the signaling pathway of Nrf2/HO-1 inhibits the degranulation of mast cells (Ye *et al.,* 2017). It is probable that HO-1 may inhibit AD and anaphylaxis. Based on these reports, we investigated the role of miR-183-5p on AD and anaphylaxis. In this study, miR-183-5p mediated AD and anaphylaxis. It would be necessary to identify cytokines and miRNAs that are regulated by miR-183-5p inhibitor.

TargetScan analysis predicted BTG-1 as a target of miR-183-5p. Downregulation of miR-183-5p inhibits growth and tube formation in vascular endothelial cells via the PI3K/Akt/VEGF signaling pathway by upregulating BTG1 (Zhang *et al.,* 2019). BTG1 acts as a negative regulator of intestinal inflammation (He *et al.,* 2017). In this study, we showed that overexpression of BTG1 inhibited in vitro allergic inflammation. The roles of BTG1 in allergic inflammations have not been reported. It would be necessary to examine whether BTG1 would affect anaphylaxis, and to identify molecules that are regulated by BTG1.

In this study, we found that miR-19a-3p was also regulated by HHT in antigen-stimulated RBL2H3 cells. MiR-19a-3p targets BTG1 and regulates apoptosis of castration-resistant prostate cancer cells (Lu *et al.,* 2015). MiR-10a-5p was also regulated by HHT in antigen-stimulated RBL2H3 cells. MiR-10a-5p acts as a negative regulator of metastatic potential of colorectal cancer cells (Liu *et al.,* 2017). It will be necessary to examine effects of miRNAs on allergic inflammations.

Curcumin could be a potential therapeutic agent for skin disorders (Vollono *et al.,* 2019). In this study, we showed that curcumin inhibited AD by regulating miR-183-5p-BTG1 axis. It also decreases the expression of thymic stromal lymphopoietin (TSLP), a cytokine implicated in the pathogenesis of asthma, AD, and anaphylaxis (Moon *et al.,*2013; Han *et al.,* 2014). EGF suppresses AD by regulating the expression of TSLP (Kim *et al.,* 2018b). TLR2 signaling increases the expression of TSLP via NF-ϰB and JNK signaling pathways in allergic airway inflammation (Lv *et al.,* 2018b). We found that TLR and TLR4 were necessary

Posted on Authorea 20 Feb 2020 — CC BY 4.0 — https://doi.org/10.22541/au.158221349.94174215 — This a preprint and has not been peer reviewed. Data may be preliminary.

for in vitro allergic inflammation (data not shown). It would be necessary to examine whether HHT and miR-183-5p-BTG1 axis would regulate the expression of TSLP.

Allergic inflammation is accompanied by an increased autophagic flux (Kim *et al.,* 2019). Autophagy is necessary for degranulation of mast cells (Nakano *et al.,* 2011). Mast cell degranulation during anaphylaxis requires ATG-7, a marker of autophagy (Ushio *et al.,*2011). It would be necessary to examine whether miR-183-5p-BTG1 axis would regulate autophagic flux during allergic inflammation.

Anaphylaxis involves cellular interactions among mast cells, macrophages, and endothelial cells (Kim *et al.,* 2019; Eom*et al.,* 2014b). In this study, we showed that AD increased the expression of CD163, but decreased the expression of iNOS. It is thus rational that AD involves interaction between mast cells and macrophages. In this study, we showed that culture medium of activated skin mast cells increased expression of CD163 and hallmarks of allergic inflammation, but decreased expression of iNOS in macrophages. This suggests that soluble factor(s) may mediate interactions between mast cells and macrophages. Exosomes mediate cellular interactions during anaphylaxis (Kim *et al.,* 2019). Exosomes of BALB/C mouse under AD might induce molecular features of AD in BALB/C mouse. Bone marrow-derived exosomes contain miR-183-5p (Davis *et al,* 2017). It would be necessary to examine the presence miR-183-5p in the exosomes of BALB/C mouse under AD and also examine exosomal miRNAs that could regulate molecular features of AD in BALB/C mouse. It is probable that HHT may prevent cellular interactions mediated by exosomes during allergic inflammations.

In this study, we showed potential of HHT as an anti-allergic drug. We also presented evidence that NF-ϰB-miR-183-5p-BTG1 axis can be employed as a target for the development of anti-allergic drugs.

Authors' contributions

Dooil Jeoung and Hyun Suk Jung conceived and designed this study. Misun Kim, Hyein Cho, and Yoojung Kwon performed experiments and analyzed the data. Dooil Jeoung and Hyun Suk Jung drafted and revised the manuscript. Youngmi Kim provided suggestion for the experiments and helped for data analysis. The manuscript has been reviewed and approved by all authors.

Conflict of Interest

The authors declare that they have no competing interests.

Acknowledgements

This work was supported by National Research Foundation Grants (2017R1A2A2A05001029, 2017M3A9G7072417, 2018R1D1A1B07043498), a grant from the BK21 plus Program.

References

Allan EK, Holyoake TL, Craig AR, Jorgensen HG (2011). Omacetaxine may have a role in chronic myeloid leukaemia eradication through downregulation of Mcl-1 and induction of apoptosis in stem/progenitor cells. Leukemia 25: 985-994.

Brunner PM, Suarez-Farinas M, He H, Malik K, Wen HC, Gonzalez J*, et al.* (2017). The atopic dermatitis blood signature is characterized by increases in inflammatory and cardiovascular risk proteins. Sci Rep 7: 8707.

Bulek K, Chen X, Parron V, Sundaram A, Herjan T, Ouyang S*, et al.*(2019). IL-17A Recruits Rab35 to IL-17R to Mediate PKCalpha-Dependent Stress Fiber Formation and Airway Smooth Muscle Contractility. J Immunol 202: 1540-1548.

Cao W, Liu Y, Zhang R, Zhang B, Wang T, Zhu X*, et al.* (2015). Homoharringtonine induces apoptosis and inhibits STAT3 via IL-6/JAK1/STAT3 signal pathway in Gefitinib-resistant lung cancer cells. Sci Rep 5: 8477.

Posted on Authorea 20 Feb 2020 — CC BY 4.0 — https://doi.org/10.22541/au.158221349.94174215 — This a preprint and has not been peer reviewed. Data may be preliminary.

Chen J, Mu Q, Li X, Yin X, Yu M, Jin J, *et al.* (2017). Homoharringtonine targets Smad3 and TGF-beta pathway to inhibit the proliferation of acute myeloid leukemia cells. *Oncotarget* 8(25): 40318-40326.

Chen XJ, Zhang WN, Chen B, Xi WD, Lu Y, Huang JY, *et al.* (2019). Homoharringtonine deregulates MYC transcriptional expression by directly binding NF-kappaB repressing factor. Proc Natl Acad Sci U S A 116: 2220-2225.

Eom S, Kim Y, Kim M, Park D, Lee H, Lee YS, *et al.* (2014). Transglutaminase II/microRNA-218/-181a loop regulates positive feedback relationship between allergic inflammation and tumor metastasis. J Biol Chem 289: 29483-29505.

Eom S, Kim Y, Park D, Lee H, Lee YS, Choe J, *et al.* (2014). Histone deacetylase-3 mediates positive feedback relationship between anaphylaxis and tumor metastasis. J Biol Chem 289: 12126-12144.

Fujimura M, Nakatsuji Y, Ishimaru H (2016). Cyclosporin A Treatment in Intrinsic Canine Atopic Dermatitis (Atopic-like Dermatitis): Open Trial Study. Pol J Vet Sci 19: 567-572.

Guttman-Yassky E, Pavel AB, Zhou L, Estrada YD, Zhang N, Xu H, *et al.* (2019). GBR 830, an anti-OX40, improves skin gene signatures and clinical scores in patients with atopic dermatitis. J Allergy Clin Immunol 144: 482-493 e487.

Han H, Thelen TD, Comeau MR, Ziegler SF (2014). Thymic stromal lymphopoietin-mediated epicutaneous inflammation promotes acute diarrhea and anaphylaxis. J Clin Invest 124: 5442-5452.

He C, Yu T, Shi Y, Ma C, Yang W, Fang L, *et al.* (2017). MicroRNA 301A Promotes Intestinal Inflammation and Colitis-Associated Cancer Development by Inhibiting BTG1. Gastroenterology 152: 1434-1448 e1415.

Hernandez-Martin A, Noguera-Morel L, Bernardino-Cuesta B, Torrelo A, Perez-Martin MA, Aparicio-Lopez C, *et al.* (2017). Cyclosporine A for severe atopic dermatitis in children. efficacy and safety in a retrospective study of 63 patients. J Eur Acad Dermatol Venereol 31: 837-842.

Huang S, Pan J, Jin J, Li C, Li X, Huang J, *et al.* (2019). Abivertinib, a novel BTK inhibitor: Anti-Leukemia effects and synergistic efficacy with homoharringtonine in acute myeloid leukemia. Cancer Lett 461: 132-143.

Jiao D, Wong CK, Qiu HN, Dong J, Cai Z, Chu M, *et al.* (2016). NOD2 and TLR2 ligands trigger the activation of basophils and eosinophils by interacting with dermal fibroblasts in atopic dermatitis-like skin inflammation. Cell Mol Immunol 13: 535-550.

Jin Y, Lu Z, Cao K, Zhu Y, Chen Q, Zhu F, *et al.* (2010). The antitumor activity of homoharringtonine against human mast cells harboring the KIT D816V mutation. Mol Cancer Ther 9: 211-223.

Kang BC, Kim MJ, Lee S, Choi YA, Park PH, Shin TY, *et al.* (2019). Nothofagin suppresses mast cell-mediated allergic inflammation. Chem Biol Interact 298: 1-7.

Kim M, Lee SH, Kim Y, Kwon Y, Park Y, Lee HK, *et al.* (2018). Human Adipose Tissue-Derived Mesenchymal Stem Cells Attenuate Atopic Dermatitis by Regulating the Expression of MIP-2, miR-122a-SOCS1 Axis, and Th1/Th2 Responses. Front Pharmacol 9: 1175.

Kim M, Park Y, Kwon Y, Kim Y, Byun J, Jeong MS, *et al.* (2019). MiR-135-5p-p62 Axis Regulates Autophagic Flux, Tumorigenic Potential, and Cellular Interactions Mediated by Extracellular Vesicles During Allergic Inflammation. Front Immunol 10: 738.

Kim TH, Jung JA, Kim GD, Jang AH, Cho JJ, Park YS, *et al.* (2010). The histone deacetylase inhibitor, trichostatin A, inhibits the development of 2,4-dinitrofluorobenzene-induced dermatitis in NC/Nga mice. Int Immunopharmacol 10: 1310-1315.

Kim Y, Kim K, Park D, Lee E, Lee H, Lee YS, *et al.* (2012). Histone deacetylase 3 mediates allergic skin inflammation by regulating expression of MCP1 protein. J Biol Chem 287: 25844-25859.

Posted on Authorea 20 Feb 2020 — CC BY 4.0 — https://doi.org/10.22541/au.158221349.94174215 — This a preprint and has not been peer reviewed. Data may be preliminary.

Kim YJ, Choi MJ, Bak DH, Lee BC, Ko EJ, Ahn GR, *et al.* (2018). Topical administration of EGF suppresses immune response and protects skin barrier in DNCB-induced atopic dermatitis in NC/Nga mice. Sci Rep 8: 11895.

Kinney SR, Carlson L, Ser-Dolansky J, Thompson C, Shah S, Gambrah A, *et al.* (2015). Curcumin Ingestion Inhibits Mastocytosis and Suppresses Intestinal Anaphylaxis in a Murine Model of Food Allergy. PLoS One 10: e0132467.

Kitayama N, Otsuka A, Nonomura Y, Nakashima C, Honda T, Kabashima K (2017). Decrease in serum IL-32 level in patients with atopic dermatitis after cyclosporine treatment. J Eur Acad Dermatol Venereol 31: e449-e450.

Ko KC, Tominaga M, Kamata Y, Umehara Y, Matsuda H, Takahashi N, *et al.* (2016). Possible Antipruritic Mechanism of Cyclosporine A in Atopic Dermatitis. Acta Derm Venereol 96: 624-629.

Krueger JG, Wharton KA, Jr., Schlitt T, Suprun M, Torene RI, Jiang X, *et al.* (2019). IL-17A inhibition by secukinumab induces early clinical, histopathologic, and molecular resolution of psoriasis. J Allergy Clin Immunol 144: 750-763.

Kwon Y, Kim Y, Eom S, Kim M, Park D, Kim H, *et al.* (2015). MicroRNA-26a/-26b-COX-2-MIP-2 Loop Regulates Allergic Inflammation and Allergic Inflammation-promoted Enhanced Tumorigenic and Metastatic Potential of Cancer Cells. J Biol Chem 290: 14245-14266.

Law Ping Man S, Bouzille G, Beneton N, Safa G, Dupuy A, Droitcourt C (2018). Drug survival and postdrug survival of first-line immunosuppressive treatments for atopic dermatitis: comparison between methotrexate and cyclosporine. J Eur Acad Dermatol Venereol 32: 1327-1335.

Lee JH, Kim JW, Ko NY, Mun SH, Her E, Kim BK, *et al.* (2008). Curcumin, a constituent of curry, suppresses IgE-mediated allergic response and mast cell activation at the level of Syk. J Allergy Clin Immunol 121: 1225-1231.

Lin CC, Law BF, Siegel PD, Hettick JM (2019). Circulating miRs-183-5p, -206-3p and -381-3p may serve as novel biomarkers for 4,4'-methylene diphenyl diisocyanate exposure. Biomarkers 24: 76-90.

Liu Y, Zhang Y, Wu H, Li Y, Zhang Y, Liu M, *et al.* (2017). miR-10a suppresses colorectal cancer metastasis by modulating the epithelial-to-mesenchymal transition and anoikis. Cell Death Dis 8: e2739.

Lu K, Liu C, Tao T, Zhang X, Zhang L, Sun C, *et al.* (2015). MicroRNA-19a regulates proliferation and apoptosis of castration-resistant prostate cancer cells by targeting BTG1. FEBS Lett 589: 1485-1490.

Lucae S, Schmid-Grendelmeier P, Wuthrich B, Kraft D, Valenta R, Linhart B (2016). IgE responses to exogenous and endogenous allergens in atopic dermatitis patients under long-term systemic cyclosporine A treatment. Allergy 71: 115-118.

Lv J, Su W, Yu Q, Zhang M, Di C, Lin X, *et al.* (2018). Heme oxygenase-1 protects airway epithelium against apoptosis by targeting the proinflammatory NLRP3-RXR axis in asthma. J Biol Chem 293: 18454-18465.

Lv J, Yu Q, Lv J, Di C, Lin X, Su W, *et al.* (2018). Airway epithelial TSLP production of TLR2 drives type 2 immunity in allergic airway inflammation. Eur J Immunol 48: 1838-1850.

Moon PD, Jeong HJ, Kim HM (2013). Down-regulation of thymic stromal lymphopoietin by curcumin. Pharmacol Rep 65: 525-531.

Nakano H, Ushio H (2011). An unexpected role for autophagy in degranulation of mast cells. Autophagy 7: 657-659.

Nguyen T, Parker R, Zhang Y, Hawkins E, Kmieciak M, Craun W, *et al.* (2018). Homoharringtonine interacts synergistically with bortezomib in NHL cells through MCL-1 and NOXA-dependent mechanisms. BMC Cancer 18: 1129.

Posted on Authorea 20 Feb 2020 — CC BY 4.0 — https://doi.org/10.22541/au.158221349.94174215 — This a preprint and has not been peer reviewed. Data may be preliminary.

Nimpong JA, Gebregziabher W, Singh UP, Nagarkatti P, Nagarkatti M, Hodge J, *et al.* (2017). Deficiency of KLF4 compromises the lung function in an acute mouse model of allergic asthma. Biochem Biophys Res Commun 493: 598-603.

Nunes FPB, Alberca-Custodio RW, Gomes E, Fonseca DM, Yokoyama NH, Labrada A, *et al.* (2019). TLR9 agonist adsorbed to alum adjuvant prevents asthma-like responses induced by Blomia tropicalis mite extract. J Leukoc Biol 106: 653-664.

Saricaoglu H, Yazici S, Zorlu O, Bulbul Baskan E, Aydogan K (2018). Cyclosporine-A for severe childhood atopic dermatitis: clinical experience on efficacy and safety profile. Turk J Med Sci *s* 48: 933-938.

Silva MJ, de Santana MBR, Tosta BR, Espinheira RP, Alcantara-Neves NM, Barreto ML, *et al.* (2019). Variants in the IL17 pathway genes are associated with atopic asthma and atopy makers in a South American population. Allergy Asthma Clin Immunol 15: 28.

Sung YY, Kim HK (2018). Crocin Ameliorates Atopic Dermatitis Symptoms by down Regulation of Th2 Response via Blocking of NF-kappaB/STAT6 Signaling Pathways in Mice. Nutrients 10.

Tao Y, Wang Y, Wang X, Wang C, Bao K, Ji L, *et al.* (2017). Calycosin Suppresses Epithelial Derived Initiative Key Factors and Maintains Epithelial Barrier in Allergic Inflammation via TLR4 Mediated NF-kappaB Pathway. Cell Physiol Biochem 44: 1106-1119.

Trian T, Allard B, Ozier A, Maurat E, Dupin I, Thumerel M, *et al.*(2016). Selective dysfunction of p53 for mitochondrial biogenesis induces cellular proliferation in bronchial smooth muscle from asthmatic patients. J Allergy Clin Immunol 137: 1717-1726 e1713.

Tsurusaki S, Tahara-Hanaoka S, Shibagaki S, Miyake S, Imai M, Shibayama S, *et al.* (2016). Allergin-1 inhibits TLR2-mediated mast cell activation and suppresses dermatitis. Int Immunol 28: 605-609.

Ushio H, Ueno T, Kojima Y, Komatsu M, Tanaka S, Yamamoto A, *et al.* (2011). Crucial role for autophagy in degranulation of mast cells. J Allergy Clin Immunol 127: 1267-1276 e1266.

Vollono L, Falconi M, Gaziano R, Iacovelli F, Dika E, Terracciano C, *et al.* (2019). Potential of Curcumin in Skin Disorders. Nutrients 11.

Wang Q, Ding W, Ding Y, Ma J, Qian Z, Shao J, *et al.* (2017). Homoharringtonine suppresses imatinib resistance via the Bcl-6/p53 pathway in chronic myeloid leukemia cell lines. Oncotarget 8: 37594-37604.

Wang Q, Gao S, Wu GZ, Yang N, Zu XP, Li WC, *et al.* (2018). Total sesquiterpene lactones isolated from Inula helenium L. attenuates 2,4-dinitrochlorobenzene-induced atopic dermatitis-like skin lesions in mice. Phytomedicine 46: 78-84.

Wu Z, Zhuang H, Yu Q, Zhang X, Jiang X, Lu X, *et al.* (2019). Homoharringtonine Combined with the Heat Shock Protein 90 Inhibitor IPI504 in the Treatment of FLT3-ITD Acute Myeloid Leukemia. Transl Oncol 12: 801-809.

Yakhni M, Briat A, El Guerrab A, Furtado L, Kwiatkowski F, Miot-Noirault E, *et al.* (2019). Homoharringtonine, an approved anti-leukemia drug, suppresses triple negative breast cancer growth through a rapid reduction of anti-apoptotic protein abundance. Am J Cancer Res 9: 1043-1060.

Ye J, Piao H, Jiang J, Jin G, Zheng M, Yang J, *et al.* (2017). Polydatin inhibits mast cell-mediated allergic inflammation by targeting PI3K/Akt, MAPK, NF-kappaB and Nrf2/HO-1 pathways. Sci Rep 7: 11895.

Yin S, Wang R, Zhou F, Zhang H, Jing Y (2011). Bcl-xL is a dominant antiapoptotic protein that inhibits homoharringtonine-induced apoptosis in leukemia cells. Mol Pharmacol 79: 1072-1083.

Zhang T, Shen S, Zhu Z, Lu S, Yin X, Zheng J, *et al.* (2016). Homoharringtonine binds to and increases myosin-9 in myeloid leukaemia. Br J Pharmacol 173: 212-221.

Posted on Authorea 20 Feb 2020 — CC BY 4.0 — https://doi.org/10.22541/au.158221349.94174215 — This a preprint and has not been peer reviewed. Data may be preliminary.

Zhang ZZ, Qin XH, Zhang J (2019). MicroRNA-183 inhibition exerts suppressive effects on diabetic retinopathy by inactivating BTG1-mediated PI3K/Akt/VEGF signaling pathway. Am J Physiol Endocrinol Metab 316: E1050-E1060.

Figure Legends

Figure 1. HHT inhibits in vitro allergic inflammation. (A) The IgE (DNP-specific)-sensitized RBL2H3 cells were treated without or with various concentrations of HHT for 1 h, followed by DNP-HSA (100 ng/ml) stimulation for 1 h. Immunoblot was performed (upper). The IgE-sensitized lung mast cells were treated without or with HHT (1 μM) for 1 h, followed by DNP-HSA stimulation for 1 h. Immunoblot was performed (lower). (B) The IgE-sensitized RBL2H3 cells were treated without or with HHT (1 μM) for 1 h, followed by DNP-HSA stimulation for 1 h. Immunoblot and immunoprecipitation were performed (right). Immunoprecipitation employing isotype-matched anti-IgG antibody was also performed. (C) The IgE-sensitized RBL2H3 cells were treated without or with HHT at the indicated concentration for 1 h, followed by DNP-HSA stimulation for 1 h. β-hexosaminidase activity assays were performed. ***, $p<0.0005$.

Figure 2. HHT inhibits PCA. (A) BALB/C mice were given an intradermal injection of DNP-specific IgE (0.5 μg/kg). The next day, BALB/C mice were given an intravenous injection of HHT (28 μg/kg) for 1 h, followed by an intravenous injection of PBS or DNP-HSA (250 μg/kg) along with 2% (v/v) Evans blue solution for determining the extent of vascular permeability accompanied by PCA. Representative images of each BALB/C mouse of each experimental group are shown. Each experimental group consisted of four BALB/C mice. Means ± S.E. of three independent experiments are depicted. **, $p<0.005$; ***, $p<0.0005$. (B) Ear tissue lysates from each mouse of each experimental group of mice were subjected to β-hexosaminidase activity assays. **, $p<0.005$; ***, $p<0.0005$. (C) Same as (B) except that immunoblot and immunoprecipitation were performed.

Figure S1. HHT inhibits PSA. (A) BALB/C mice were given an intravenous injection of DNP-specific IgE (0.5 μg/kg). The next day, BALB/C mice were given an intravenous injection of HHT (28 μg/kg) for 1 h, followed by an intravenous injection of DNP-HSA (250 μg/kg). At each time point after injection with DNP-HSA, rectal temperatures were measured. Each experimental group consisted of five mice. *, $p<0.05$; **, $p<0.005$; ***, $p<0.0005$, compared with IgE/PBS; #, $p<0.05$; ##, $p<0.005$, compared with IgE/PBS/DNP-HSA. (B) β-hexosaminidase activity assays were performed . ***, $p<0.0005$. (C) Same as (B) except that immunoblot and immunoprecipitation were performed. (D) Immunohistochemical staining employing lung tissue was performed. Quantification was performed by calculating the percentage of the staining intensities using Image J (NIH). **, $p<0.005$.

Figure 3. HHT attenuates clinical symptoms associated with AD.(A) 2, 4-dinitro fluorobenzene (DNFB) induced AD. HHT (28 μg/kg) was intravenously injected at the indicated days of the time line. Clinical scores of BALB/C mice of each experimental group were determined as described. *, $P<0.05$; ***, $p<0.0005$. (B) Tissue lysates from each mouse of each experimental group of mice were subjected to β-hexosaminidase activity assays. ***, $p<0.0005$. (C) Sera of BALB/C mice of each experimental group were employed for the determination of the amount of histamine released. *$p < 0.05$; **, $p < 0.005$. (D) Same as (B) except that immunoblot and immunoprecipitation were performed. (E) Same as (D) except that lysates of skin mast cells isolated from skin tissue were employed. (F) Skin tissue lysates were subjected to qRT-PCR analysis.

Figure S2. HHT inhibits molecular and cellular features of AD.(A) Immunohistochemical staining was performed as described. Quantification was performed by calculating the percentage of the staining intensities using Image J (NIH). *, $P<0.05$; **, $p<0.005$; ***, $p<0.0005$. (B) H&E staining was performed to examine the extent of epithelial hyperplasia (upper). Toluidine blue staining was performed to examine the number of activated mast cells (lower). Red arrows denote activated mast cells. Red rectangle is an enlarged version of activated mast cells (red circle). Black rectangle is an enlarged version of mast cells (black circle).

Figure S3. DNFB induces features of allergic inflammation . RBL2H3 cells were pretreated without

Posted on Authorea 20 Feb 2020 — CC BY 4.0 — https://doi.org/10.22541/au.158221349.94174215 — This a preprint and has not been peer reviewed. Data may be preliminary.

or with HHT (1 μM) for 1 h, followed by DNFB (100 nM) treatment for 1 h. Immunoblot and immunoprecipitation were performed.

Figure S4. HHT prevents antigen from regulating expression levels of TH1/TH2 cytokines and FoxP3 in AD . Tissue lysates from each mouse of each experimental group were subjected to qRT-PCR analysis. *p < 0.05; **, p < 0.005; ***, p<0.0005.

Figure 4. MiR-183-5p mediates in vitro allergic inflammation.(A) The IgE-sensitized RBL2H3 cells were treated without or with HHT (1 μM) for 1h, followed by DNP-HSA stimulation for 1 h. MiRNA array analysis was performed. (+) represents increase in expression level of the indicated miRNA in RBL2H3 cells. (-) represents decrease in expression level of the indicated miRNA in RBL2H3 cells. (B) The IgE-sensitized RBL2H3 cells or lung mast cells were treated without or with HHT (1 μM) for 1h, followed by DNP-HSA stimulation for 1 h. QRT-PCR analysis was performed. *p < 0.05; **, p < 0.005. (C) RBL2H3 cells were transfected with the indicated inhibitor (each at 10 nM). The next day, cells were sensitized with IgE for 24 h, followed by DNP-HSA stimulation for 1 h. β-hexosaminidase activity assays and qRT-PCR analysis were performed. *p < 0.05; **, p < 0.005; ***, p<0.0005. (D) Same as (C) except that immunoblot and immunoprecipitation were performed.

Figure 5. MiR-183-5p mediates PCA. (A) BALB/C mice were given an intradermal injection of DNP-specific IgE antibody (0.5 μg/kg) or IgG (0.5 μg/kg) along with the indicated inhibitor (each at 100 nM). The next day, BALB/C mice were given an intravenous injection of PBS or DNP-HSA (250 μg/kg) along with 2% (v/v) Evans blue solution. Each experimental group consisted of four BALB/C mice. Means ± S.E. of three independent experiments are depicted. (B) qRT-PCR and β-hexosaminidase activity assays were performed. *p < 0.05; ***, p<0.0005. (C) Immunoblot and immunoprecipitation were performed.

Figure S5. MiR-183-5p mediates PSA. (A) BALB/C mice were given an intradermal injection of DNP-specific IgE antibody (0.5 μg/kg) or IgG (0.5 μg/kg) along with the indicated inhibitor (each at 100 nM). The next day, BALB/C mice were given an intravenous injection of PBS or DNP-HSA (250 μg/kg). Each experimental group consisted of four BALB/C mice. ***, p<0.0005, compared with IgE/Ctrl. Inh./PBS; #, p<0.05; ##, p<0.005, compared with IgE/Ctrl. Inh./DNP-HSA. (B) β-hexosaminidase activity assays and qRT-PCR analysis were performed. Serum of each BALB/C mouse of each experimental group was employed to determine the amount of histamine released. **p < 0.005; ***, p<0.0005. (C) Immunoblot and immunoprecipitation were performed.

Figure 6. MiR-183-5p mediates AD. (A) AD was induced. The indicated inhibitor (each at 100 nM) was intravenously injected at the indicated days. (B) At the indicated day (day 20) after the induction of AD, clinical scores of BALB/C mice of each experimental group were determined (upper panel). β-hexosaminidase activity assays were performed (lower panel). *p < 0.05; **, p < 0.005; ***, p<0.0005. (C) Immunoblot and immunoprecipitation were performed. (D) QRT-PCR analyses were performed. *p < 0.05; **, p < 0.005; ***, p<0.0005.

Figure S6. MiR-183-5p inhibitor negatively regulates features of AD. (A) Immunohistochemical staining of skin tissue of each mouse of each experimental group was performed. Quantification was performed by calculating the percentage of the staining intensities using Image J (NIH). **, p < 0.005; ***, p<0.0005. (B) H&E staining (upper panel) and toluidine blue staining (lower panel) were performed. Red arrows denote activated mast cells. Red rectangle is an enlarged version of activated mast cells (red circle). Black rectangle is an enlarged version of mast cells (black circle).

Figure S7. MiR-183-5p and NF-kB form positive feedback loop to mediate allergic inflammation. (A) Skin tissue lysates from BALB/C mouse under AD without or with HHT (left) or BALB/C mouse under AD with the injection of the indicated inhibitor (middle) were subjected to immunoblot (middle). RBL2H3 cells were treated without or with HHT (1 μM) for 1 h, followed by DNFB (100 μM) treatment for 1 h (right). (B) RBL2H3 cells were treated without or with HHT for 1 h, followed by DNFB treatment for 1 h. Immunofluorescence staining was performed. (C) The IgE-sensitized RBL2H3 cells were stimulated with DNP-HSA for 1 h, followed by ChIP assays. Numbers in parentheses denote PCR-amplified regions.

Posted on Authorea 20 Feb 2020 — CC BY 4.0 — https://doi.org/10.22541/au.158221349.94174215 — This a preprint and has not been peer reviewed. Data may be preliminary.

Figure S8. MiR-183-5p directly targets BTG1. (A) Potential binding of miR-183-5p to the 3'-UTR of BTG1 was shown. Wild type Luc-BTG1-3'-UTR or mutant Luc-BTG1-3'-UTR was transfected along with the indicated inhibitor (each at 10 nM) into the indicated cell line. At 48 h after transfection, luciferase activity assays were performed. *p < 0.05; **p < 0.005. (B) Skin tissue lysates from BALB/C mice under AD were subjected to immunoblot. (C) The IgE-sensitized RBL2H3 cells were pretreated without or with HHT at the indicated concentration for 1 h, followed by stimulation with DNP-HSA for 1 h.

Figure 7. BTG1 inhibits in vitro allergic inflammation. (A) RBL2H3 cells were transfected with control vector (1 μg) or Flag-BTG1 (1 μg). The next day, cells were then sensitized with anti-IgE antibody (100 ng/ml) for 24 h, followed by stimulation with DNP-HSA for 1 h. Immunoblot and immunoprecipitation were performed. (B) β-hexosaminidase activity assays and qRT-PCR analysis were performed. **, p<0.005; ***, p<0.0005. (C) HaCaT cells were transfected with the indicated construct (each at 1 μg). The next day, cells were treated without or with DNFB for 1 h, followed by immunoblot and qRT-PCR analysis. *, p<0.05; ***, p<0.0005.

Φιγυρε 8. ΝΦ-κΒ ις νεςεσσαρψ φορ ιν ιτρο αλλεργις ινφλαμματιον. (A) The IgE-sensitized RBL2H3 cells were pretreated without or with BAY 11-0782 (20 μM) for 1h, followed by stimulation with DNP-HSA for 1 h. (B) Same as (A) except that qRT-PCR analysis and β-hexosaminidase activity assays were performed. **, p<0.005; ***, p<0.0005. (C) immunofluorescence staining was performed. (D) HaCaT cells were pretreated without or with BAY 11-0782 (1 μM) for 1h, followed by stimulation with DNFB for 1 h. Immunoblot and qRT-PCR analysis were performed. *, p<0.05; **, p<0.005; ***, p<0.0005.

Figure S9. NF-kB mediates PCA. (A) BALB/C mice were given an intradermal injection of DNP-specific IgE antibody (0.5 μg/kg) or IgG (0.5 μg/kg). The next day, BALB/C mice were given an intravenous injection of PBS or DNP-HSA (250 μg/kg) along with BAY 11-0782 (1 mg/kg) along with 2% (v/v) Evans blue solution. Each experimental group consisted of four BALB/C mice. Means ± S.E. of three independent experiments are depicted. (B) β-hexosaminidase activity assays and qRT-PCR analysis were performed. *, p<0.05; **p < 0.005; ***, p<0.0005. (C) Immunoblot and immunoprecipitation were performed. (D) HaCaT cells were pretreated without or with BAY 11-0782 (1 μM) for 1 h, followed by stimulation with DNFB for 1 h.

Figure S10. Curcumin inhibits in vitro allergic inflammation.(A) The IgE-sensitized RBL2H3 cells were pretreated without or with curcumin (10 μM) for 1 h, followed by stimulation with DNP-HSA for 1h. Immunoblot and qRT-PCR were performed. *, p<0.05; ***, p<0.0005. (B) RBL2H3 cells were treated with DNFB for 1 h, followed by treatment with various concentration of curcumin for 1 h, followed by immunoblot and immunoprecipitation. (C) Same as (A) except that immunofluorescence staining was performed. (D) RBL2H3 cells were treated with DNFB for 1 h, followed by treatment with curcumin (10 μM) for 1 h. (D) HaCaT cells were treated without or with DNFB (100 μM) for 1 h, followed by treatment with curcumin (10 μM) for 1 h. Immunoblot and qRT-PCR analysis were performed. ***, p<0.0005.

Figure 9. Curcumin inhibits AD. (A) AD was induced. BALB/C mice were given an intraperitoneal injection of curcumin (50mg/kg) at the indicated days of the time line (upper panel). Clinical scores of BALB/C mice of each experimental group were determined. *, P<0.05; **, p<0.005. (B) β-hexosaminidase activity assays and qRT-PCR analysis were performed. **p < 0.005; ***, p < 0.0005. (C) Same as (B) except that immunoblot and immunoprecipitation were performed.

Figure S11. Curcumin inhibits features of AD. (A) Immunohistochemical staining of skin tissue of each mouse of each experimental group of mice was performed. Quantification was performed by calculating the percentage of the staining intensities using Image J (NIH). *, p < 0.05; **, p<0.005. (B) H&E staining (upper panel) and toluidine blue staining (lower panel) were performed.

Red arrows denote activated mast cells. Red rectangle is an enlarged version of mast cells (red circle). Black rectangle is an enlarged version of mast cells (black circle).

Figure 10. HHT regulates cellular interactions in atopic dermatitis. (A) The culture medium of

Posted on Authorea 20 Feb 2020 — CC BY 4.0 — https://doi.org/10.22541/au.158221349.94174215 — This a preprint and has not been peer reviewed. Data may be preliminary.

skin mast cells isolated from BALB/C mouse of each experimental group was added to lung macrophages for 8 h. C.M. denotes culture medium. (B) Same as (A) except that immunofluorescence staining was performed.

Figure S12. Curcumin and miR-183-5p inhibitor inhibit cellular interactions during AD. (A) The culture medium of skin mast cells isolated from BALB/C mouse of each experimental group was added to lung macrophages for 8 h. (B) The culture medium of skin mast cells isolated from BALB/C mouse of each experimental group was added to lung macrophages for 8 h, followed by immunoblot. (C) Same as (A) except that immunofluorescence staining was performed. (D) Same as (B) except that immunofluorescence staining was performed.

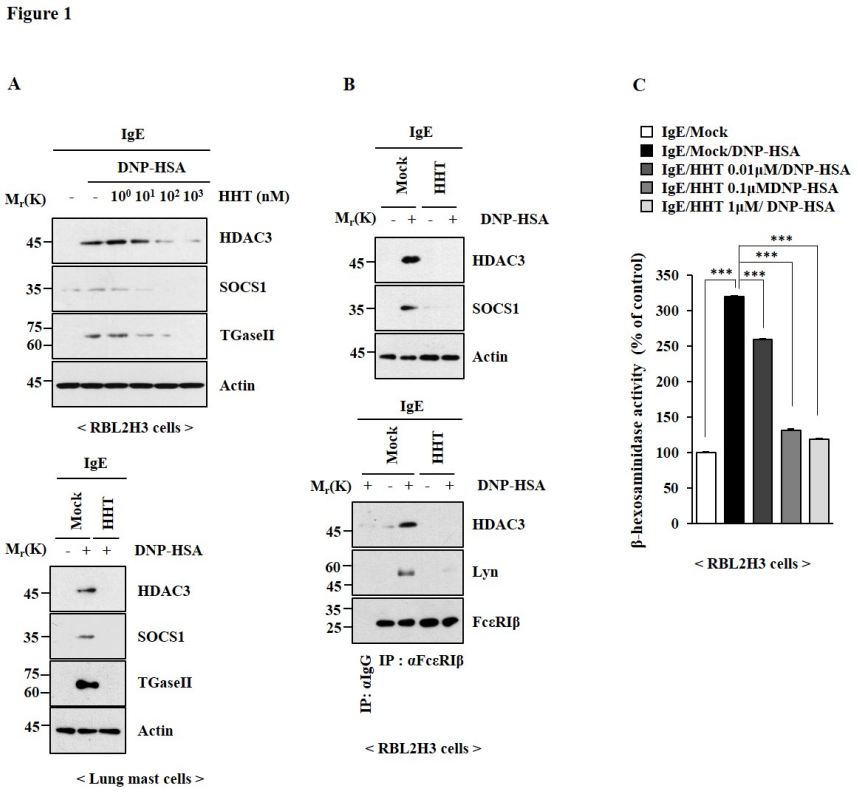

Posted on Authorea 20 Feb 2020 — CC BY 4.0 — https://doi.org/10.22541/au.158221349.94174215 — This a preprint and has not been peer reviewed. Data may be preliminary.

Posted on Authorea 20 Feb 2020 — CC BY 4.0 — https://doi.org/10.22541/au.158221349.94174215 — This a preprint and has not been peer reviewed. Data may be preliminary.

Figure 2

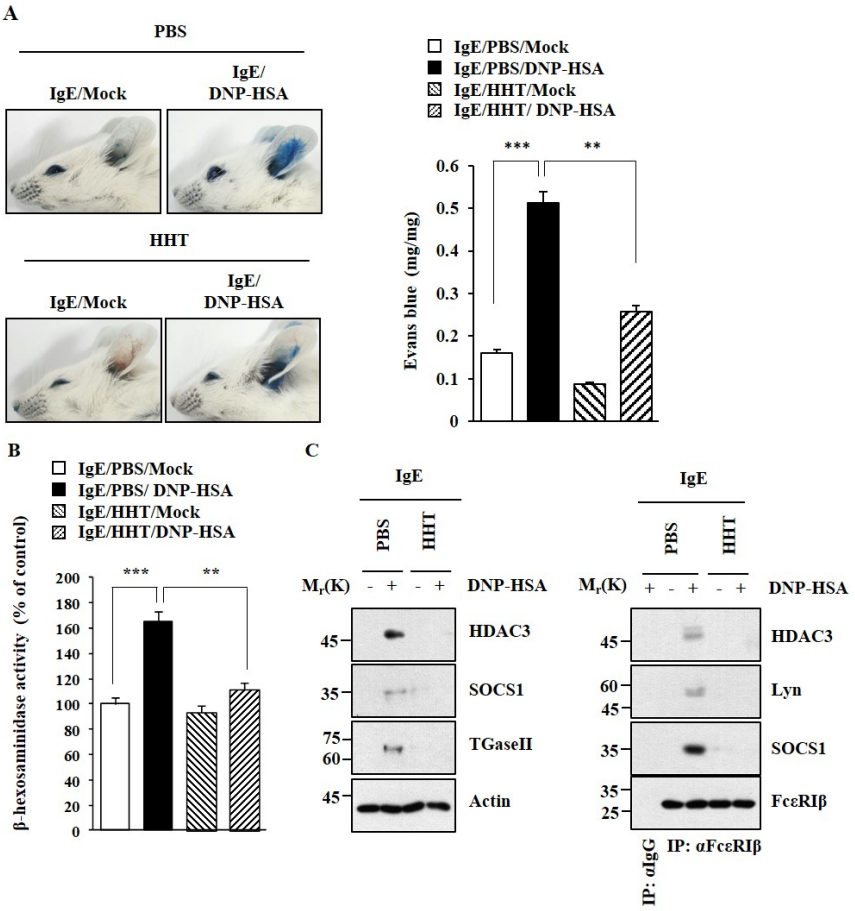

Posted on Authorea 20 Feb 2020 — CC BY 4.0 — https://doi.org/10.22541/au.158221349.94174215 — This a preprint and has not been peer reviewed. Data may be preliminary.

Figure 3

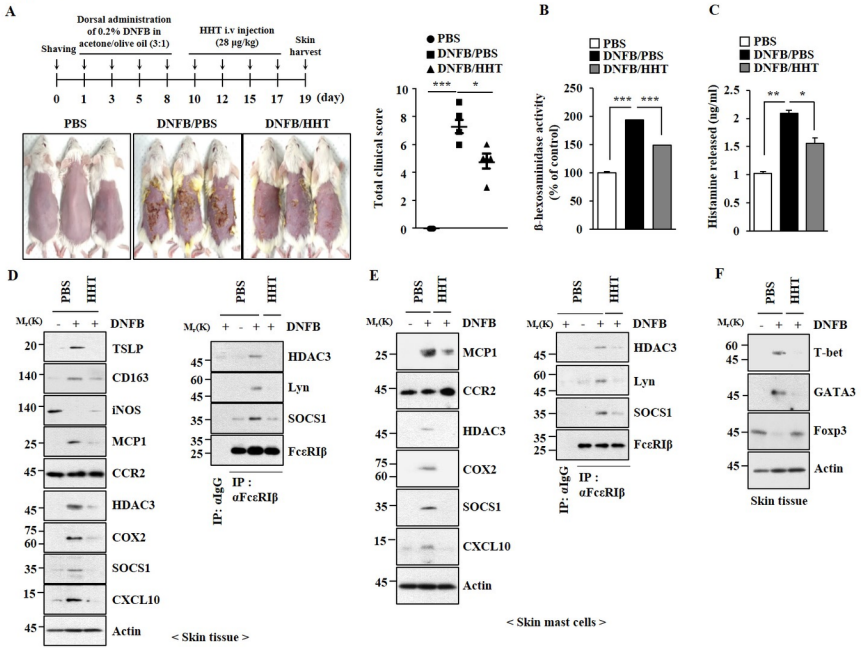

Figure 4

A

miRNAs	Fold changes	
	IgE/Mock vs IgE/DNP-HSA	IgE/DNP-HSA vs IgE/HHT/DNP-HSA
miR-10a-5p	+ 3.92	-2.40
miR-19a-3p	+ 5.83	-5.75
miR-134-5p	+ 9.28	-8.70
miR-183-5p	+ 6.05	-9.55
miR-100-5p	+ 2.33	-8.59
miR-182-5p	-4.94	+ 5.33
miR-204-5p	-5.84	+ 4.35
miR-219	-7.30	+ 7.04

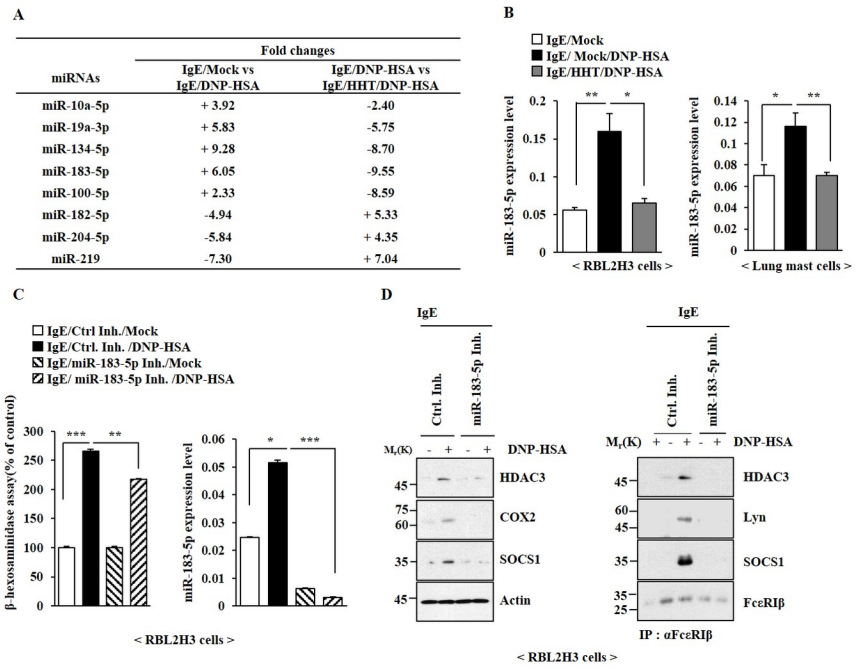

Posted on Authorea 20 Feb 2020 — CC BY 4.0 — https://doi.org/10.22541/au.158221349.94174215 — This a preprint and has not been peer reviewed. Data may be preliminary.

Figure 5

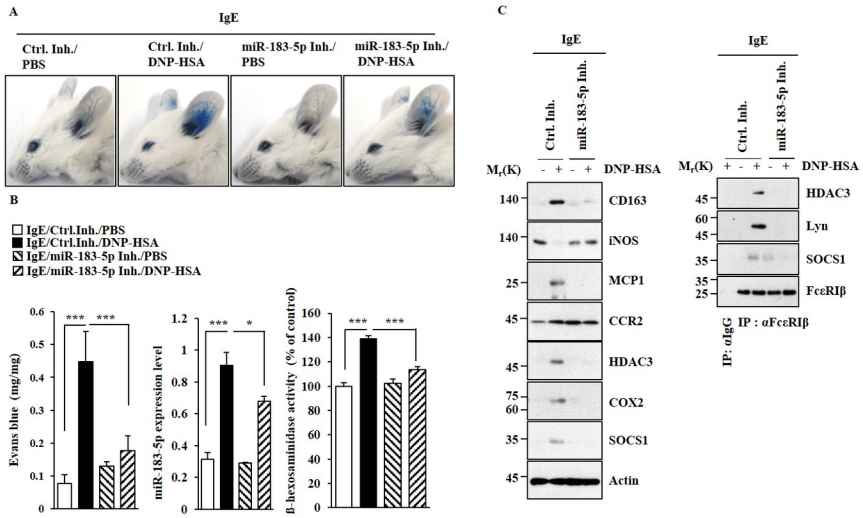

Figure 6

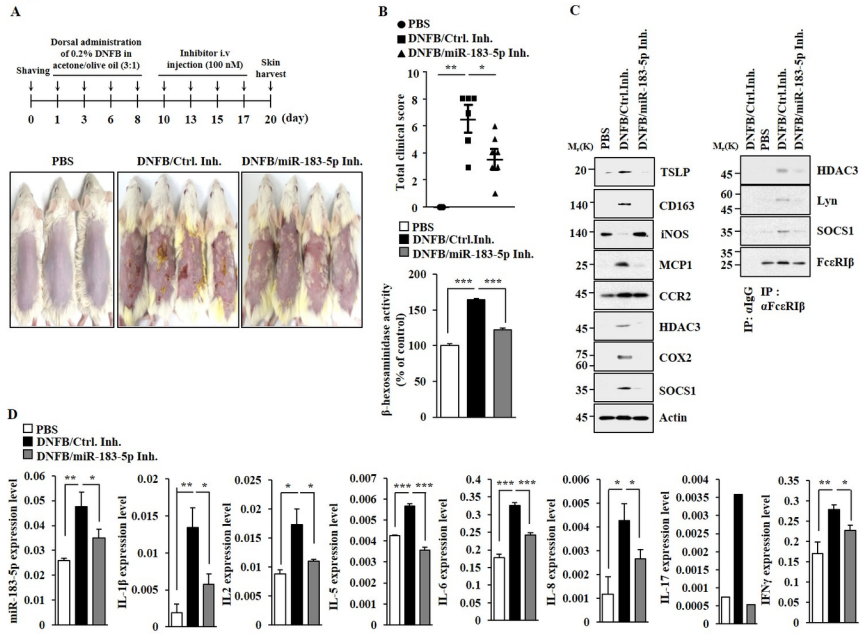

Posted on Authorea 20 Feb 2020 — CC BY 4.0 — https://doi.org/10.22541/au.158221349.94174215 — This a preprint and has not been peer reviewed. Data may be preliminary.

Figure 7

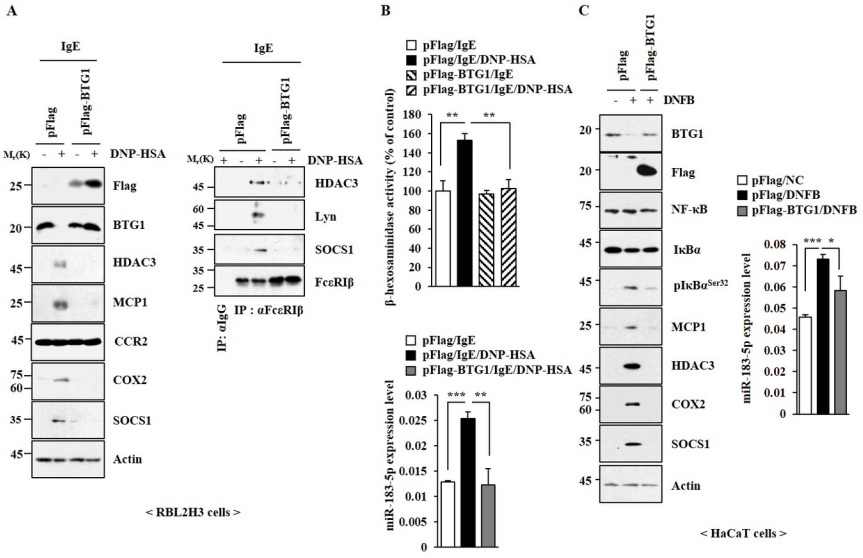

Figure 8

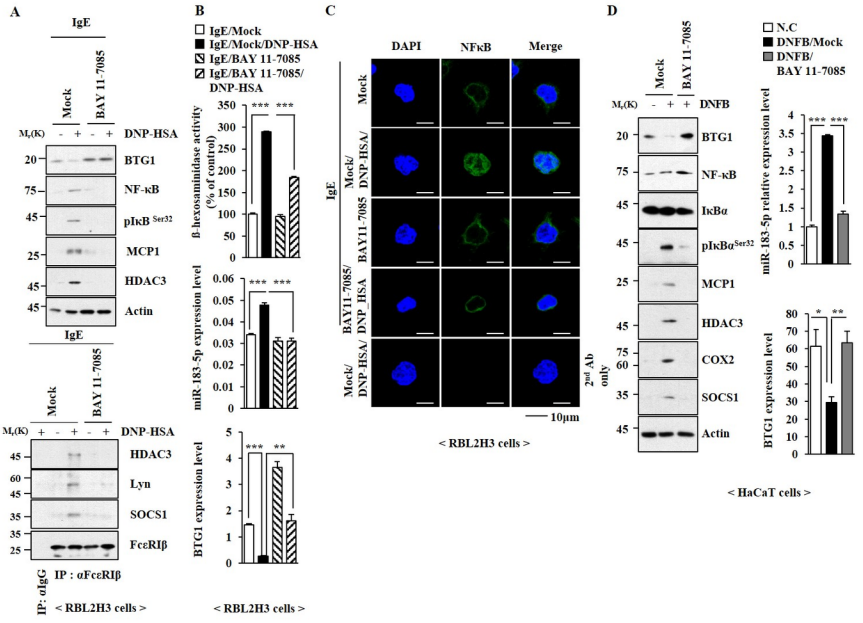

Figure 9

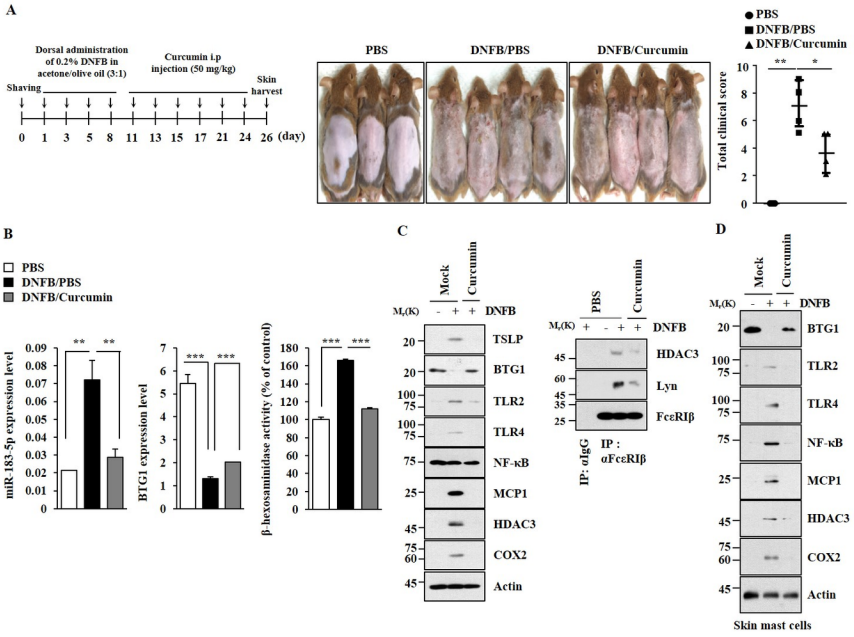

Figure 10

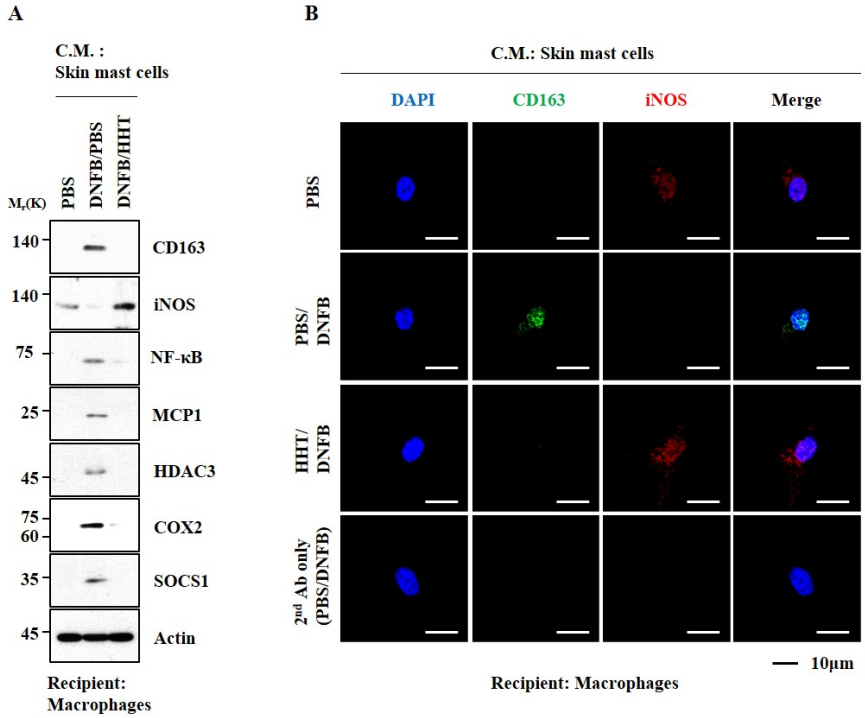

Posted on Authorea 20 Feb 2020 — CC BY 4.0 — https://doi.org/10.22541/au.158221349.94174215 — This a preprint and has not been peer reviewed. Data may be preliminary.